S. Afr. J. Chem., 2014, **67**, 91–93,
<http://journals.sabinet.co.za/sajchem/>.

Synthesis and Structural Studies of Nanocrystalline $Cd_{0.3}Zn_{0.7}Fe_2O_4$

Kalpanadevi Kalimuthu, Sinduja C. Rangasamy and Manimekalai Rakkiyasamy*

Department of Chemistry, Kongunadu Arts and Science College, Coimbatore, Tamilnadu, India, PIN – 641 029.

Received 9 January 2014, revised 17 February 2014, accepted 19 June 2014.

ABSTRACT

The synthesis of $Cd_{0.3}Zn_{0.7}Fe_2O_4$ nanoparticles has been achieved by a simple thermal decomposition method from the inorganic precursor, $Cd_{0.3}Zn_{0.7}Fe_2(cin)_3(N_2H_4)_2$, which was obtained by a novel precipitation method from the corresponding metal salts, cinnamic acid and hydrazine hydrate. The precursor was characterized by hydrazine and metal analyses, infrared spectral analysis and thermogravimetric analysis. Under appropriate annealing conditions, $Cd_{0.3}Zn_{0.7}Fe_2(cin)_3(N_2H_4)_2$ yielded $Cd_{0.3}Zn_{0.7}Fe_2O_4$ nanoparticles, which were characterized for their size and structure using X-Ray Diffraction (XRD), High Resolution Transmission Electron Microscopic (HRTEM), Selected Area Electron Diffraction (SAED) and Scanning Electron Microscopic (SEM) techniques.

KEYWORDS

$Cd_{0.3}Zn_{0.7}Fe_2O_4$ nanoparticles, XRD, HRTEM, SAED, SEM.

1. Introduction

Spinel ferrites in nanoscale are gaining eminence due to their effectual properties such as high thermodynamic stability, high electrical conductivity, and high corrosion resistance, making them suitable in metallurgical field and other high temperature areas. Zinc ferrite ($ZnFe_2O_4$), an important spinel ferrite, is a commercially important material and has been widely used in a number of applications.[1–6] Various methods have been developed to synthesize nanocrystalline $ZnFe_2O_4$.[7–12]. Among these established methods, thermal treatment is the most important as it ensures smaller particle-size product of high purity, high crystallinity, chemical homogeneity and better yield, and is a low-cost technique especially suitable for mass production of the pure and doped spinel ferrite nanopowders.

There is ample literature on the synthesis and characterization of zinc ferrite nanoparticles. Recently, we have been successful in synthesizing nanocrystalline $ZnFe_2O_4$ through the thermal decomposition of the corresponding inorganic precursor.[13] There are merely a very few reports on the synthesis of cadmium substituted zinc ferrite by various other methods.[14,15] Therefore, an attempt has been made in the present work to synthesize nanocrystalline $Cd_{0.3}Zn_{0.7}Fe_2O_4$ by thermal decomposition route.

2. Experimental

2.1. Preparation and Characterization of the Precursor $Cd_{0.3}Zn_{0.7}Fe_2(cin)_3(N_2H_4)_2$

$Cd_{0.3}Zn_{0.7}Fe_2(cin)_3(N_2H_4)_2$ was prepared by the addition of an aqueous solution (50 mL) of hydrazine hydrate (1.6 mL, 0.02 mol) and cinnamic acid (1.18 g, 0.0079 mol) to the corresponding aqueous solution (50 mL) of cadmium nitrate hexahydrate (0.3 g, 0.0009 mol), zinc nitrate hexahydrate (0.7 g, 0.0023 mol) and ferrous sulphate heptahydrate (1.11 g, 0.0039 mol). The brown orange product formed immediately was kept aside for an hour, then filtered and washed with water, alcohol followed by diethylether and air dried.

The hydrazine content in the precursor was determined by titration using KIO_3 as the titrant under Andrew's conditions.[16] The percentage of cadmium, zinc and iron in the precursor was estimated by gravimetry as given in the Vogel's textbook.[16] The infrared spectrum of the solid precursor sample was recorded by the KBr disc technique using a Shimadzu spectrophotometer (IRTracer-100). The simultaneous TG-DSC experiment was carried out in Universal V4.5A TA Instrument, in nitrogen atmosphere at the heating rate of 20 °C per minute using 510 mg of the sample. The temperature range was ambient to 700 °C.

* To whom correspondence should be addressed. E-mail: manimekalaikasc@gmail.com

2.2. Preparation and Characterization of $Cd_{0.3}Zn_{0.7}Fe_2O_4$ Nanoparticles

$Cd_{0.3}Zn_{0.7}Fe_2O_4$ nanoparticles were obtained from the autoatalytic decomposition of the precursor. In this method, the dried precursor was transferred to a silica crucible and heated to red-hot condition in an ordinary atmosphere for about 45 minutes. The precursor started decomposing violently. The total decomposition of $Cd_{0.3}Zn_{0.7}Fe_2(cin)_3(N_2H_4)_2$ led to the formation of $Cd_{0.3}Zn_{0.7}Fe_2O_4$, which were cooled to room temperature, ground well in a mortar and stored.

The size and structure of the synthesized nanoparticles were determined by High Resolution Transmission Electron Microscopy (HRTEM) operating on Jeol Jem 2100 advanced analytical electron microscope. Scanning electron microscopy (SEM) was performed with a HITACHI Model S-3000H by focusing on nanoparticles to study the morphology. To check phase formation and purity, XRD pattern was recorded using an X-ray diffractometer (X'per PRO model) using CuKa radiation, at 40 keV.

3. Results and Discussion

3.1. Chemical Formula Determination of the Precursor

Based on the observed percentage of hydrazine (9.35), cadmium (12.90), zinc (17.31) and iron (42.98) which are found to match closely with the calculated values (9.60), (13.21), (17.92) and (43.76) for hydrazine, cadmium, zinc and iron, respectively, the chemical formula $Cd_{0.3}Zn_{0.7}Fe_2(cin)_3(N_2H_4)_2$ has been tentatively assigned to the precursor.

3.2. IR Spectral Analysis of the Precursor

The IR spectrum of $Cd_{0.3}Zn_{0.7}Fe_2(cin)_3(N_2H_4)_2$ exhibited a strong band at 972 cm^{-1} due to the N-N stretching frequency, which explicitly proved the bridging nature of the hydrazine moieties.[17] The asymmetric and symmetric stretching frequencies of the carboxylate ions were seen at 1639 and 1411 cm^{-1}, respectively, with the $\Delta\upsilon_{(\upsilon_{asymm}\text{-}\upsilon_{sym})}$ separation of 228 cm^{-1}, which indicated the monodentate linkage of the carboxylate groups. The N-H stretching was observed at 3363 cm^{-1}.

3.3. Thermal Analysis of the Precursor

The TG-DSC curve in Fig. 1 shows that the precursor loses weight in three particular steps. The first step is the dehydrazination, which is the removal of hydrazine molecules from the precursor, taking place between room temperature and 190 °C with a weight loss of 5%. The corresponding peak in DSC is observed as an endotherm. The second and third steps are attributed to the decarboxylation of the dehydrazinated precursor, which gives $Cd_{0.3}Zn_{0.7}Fe_2O_4$ as the final residue.

3.4. Characterization of $Cd_{0.3}Zn_{0.7}Fe_2O_4$ Nanoparticles

3.4.1. *XRD Analysis*

The diffraction pattern shown in Fig. 2 corresponds to that of the as-synthesized $Cd_{0.3}Zn_{0.7}Fe_2O_4$ nanoparticles. The broadening nature of the peaks indicates that the crystallite size of the sample is within the nanometer scale. The average crystallite size estimated using Debye-Scherrer formula, $D = K\lambda/\beta\cos\theta$, where, θ is Bragg diffraction angle, K is Blank's constant, λ is the source wavelength (1.54), and β is the width of the XRD peak at half maximum height is found to be around 20 nm. No characteristic peaks for other impurities are detected, confirming that the product obtained is phase pure.

3.4.2. *HRTEM Analysis*

HRTEM micrograph of $Cd_{0.3}Zn_{0.7}Fe_2O_4$ in Fig. 3 shows that most of the nanoparticles are sphere-shaped. A slight aggregation is visible which is probably due to the aggregation or overlapping of some small individual particles, owing to their magnetic induction. The average grain size observed from the micrograph is about 19–20 nm, which is in concurrence with the calculation using Scherrer's formula. Figure 4 shows the selected area electron diffraction (SAED) pattern indicating sharp rings, which reveal the polycrystalline nature of the nanoparticles.

3.4.3. *SEM Analysis*

The SEM picture in Fig. 5 clearly shows randomly distributed grains with fairly uniform size. A large agglomeration of particles is noticeable which may be due to their magnetic interaction.

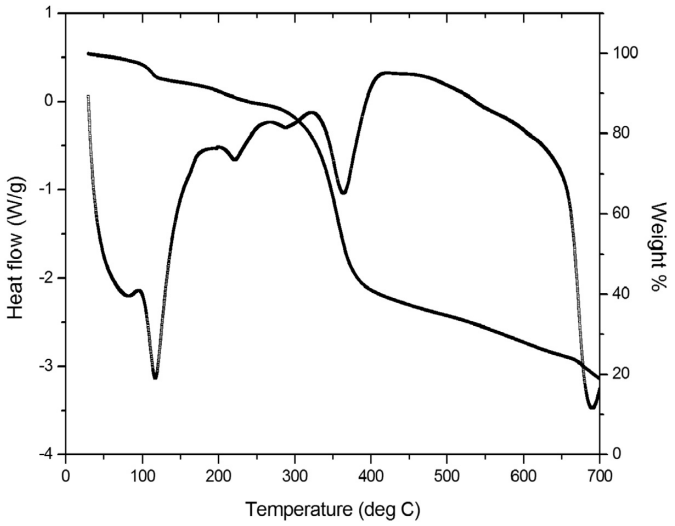

Figure 1 TG-DSC curve of $Cd_{0.3}Zn_{0.7}Fe_2(cin)_3(N_2H_4)_2$.

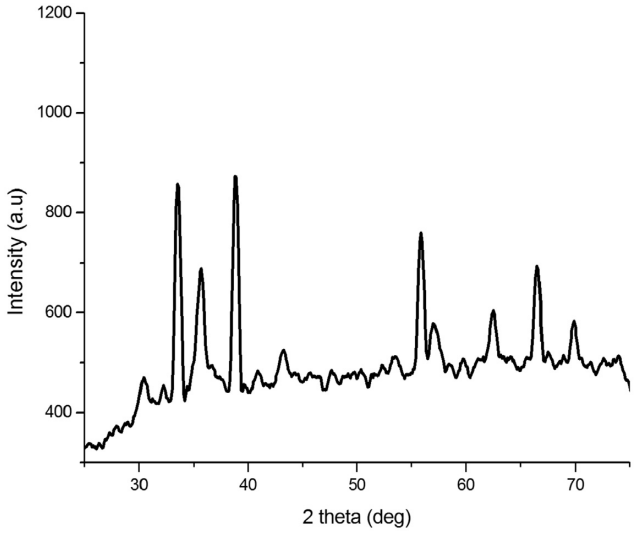

Figure 2 XRD pattern of $Cd_{0.3}Zn_{0.7}Fe_2O_4$ nanoparticles.

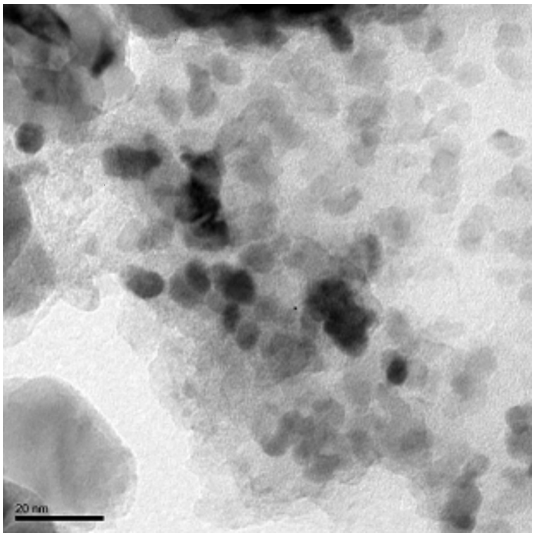

Figure 3 HRTEM image of $Cd_{0.3}Zn_{0.7}Fe_2O_4$ nanoparticles.

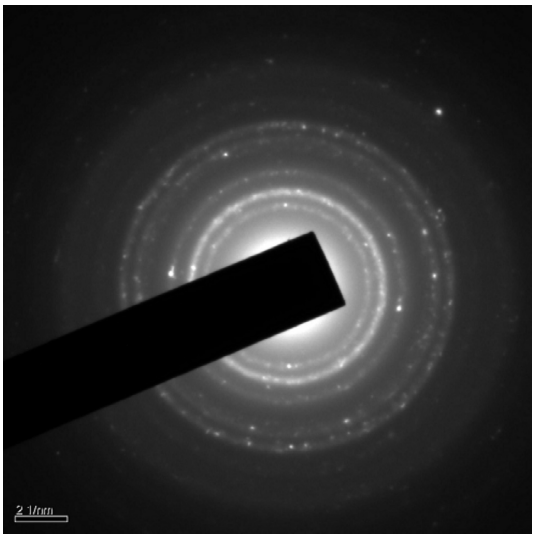

Figure 4 SAED pattern of $Cd_{0.3}Zn_{0.7}Fe_2O_4$ nanoparticles.

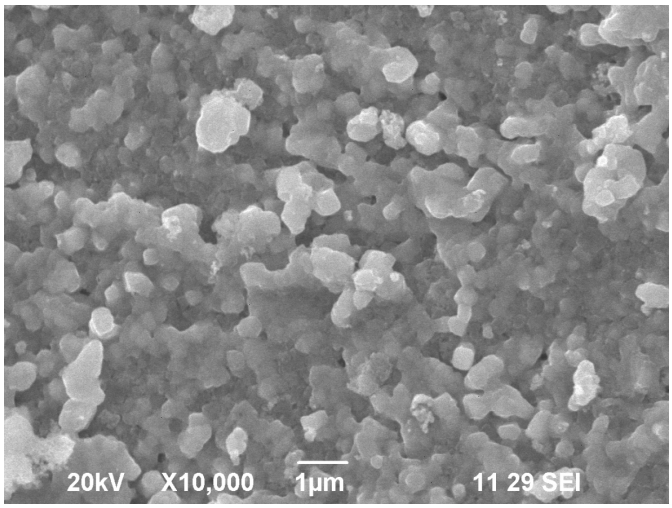

Figure 5 SEM image of $Cd_{0.3}Zn_{0.7}Fe_2O_4$ nanoparticles.

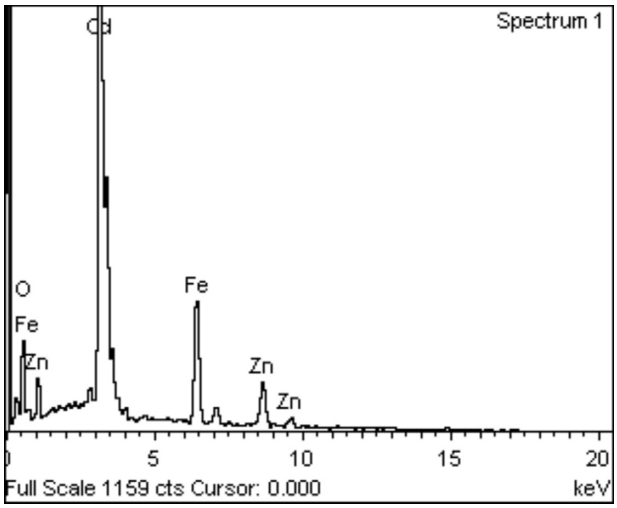

Figure 6 EDX spectrum of $Cd_{0.3}Zn_{0.7}Fe_2O_4$ nanoparticles.

EDX spectrum of $Cd_{0.3}Zn_{0.7}Fe_2O_4$ nanoparticles is presented in Fig. 6, which furnishes the chemical compositional analysis of the nanoscale $Cd_{0.3}Zn_{0.7}Fe_2O_4$.

4. Conclusions

Nanocrystalline $Cd_{0.3}Zn_{0.7}Fe_2O_4$ was prepared by using a simple and novel thermal decomposition method and characterized for their size and structure by XRD, HRTEM, SAED and SEM techniques. The average particle size of $Cd_{0.3}Zn_{0.7}Fe_2O_4$ nanoparticles determined from XRD and HRTEM is about 20 nm. SEM image reveals that the sample consists of grains of almost spherical shape.

References

1 H. Deng, X. Li, Q. Peng, X. Wang, J. Chen and Y. Li, *Angew. Chem., Int. Ed. Engl.*, 2005, **44**, 2782–2785.

2 Niu, W. Du and W. Du, *Sens. Actuators, B, Chem.*, 2004, **99**, 405–409.

3 J.A. Toledo-Antonio, N. Nava, M. Martínez and X. Bokhimi, *Appl. Catal., A Gen.*, 2002, **234**, 137–144.

4 J. Qiu, C. Wang and M. Gu, *Mater. Sci. Eng., B, Solid-State Mater. Adv.Technol.,* 2004, **112**, 1–4.

5 F. Tomás-Alonso and J.M. Palacios Latasa, *Fuel Process. Technol.*, 2004, **86**, 191–203.

6 L.J. Love, J.F. Jansen, T.E. McKnight, Y. Roh, T.J. Phelps, L.W. Yeary and G.T. Cunningham, *IEEE, Mechatronics,* 2005, **10**, 68–76.

7 Y. Shi, J. Ding, S.L.H. Tan and Z. Hu, *J Magn. Magn. Mater.*, 2003, **256**, 13–19.

8 Y. Kinemuchi, K. Ishizaka, H. Suematsu, W. Jiang and K. Yatsui, *Thin Solid Films,* 2002, **407**, 109–113.

9 D.H. Chen and X.R. He, *Mater. Res. Bull.*, 2001, **36**, 1369–1377.

10 C. Liu, B. Zou, A.J. Rondinone and Z.J. Zhang, *J. Phys. Chem.,* 2000, **B104**, 1141–1145.

11 H.M. Fan, J.B. Yi, Y. Yang, K.W. Kho, H.R. Tan and Z.X. Shen, *et al.*, *ACS Nano,* 2009, **3**, 2798–2808.

12 H. Li, H.Z. Wu and G.X. Xiao, *Powder Technol.,* 2010, **198**, 157–166.

13 K. Kalpanadevi, C.R. Sinduja and R. Manimekalai, *Acta Chim. Slov.,* 2013, **60**, 896–900.

14 C. Otero Arean, E. Garcia Diaz, J.M. Rubio Gonzalez and M.A. Villa Garcia, *J. Solid State Chem.,* 1988, **77**, 275–280.

15 S. Ghatak, G. Chakraborty, M. Sinha, S. Kumar Pradan and A. Kumar Meikap, *Mater. Sci. Appl.,* 2011, **2**, 226–236.

16 I. Vogel, *A Textbook of Quantitative Inorganic Analysis*, 4th edn., Longman, UK, 1985.

17 A. Braibanti, F. Dallavalle, M.A. Pellinghelli and E. Leporati, *Inorg. Chem.*, 1968, **7**, 1430–1433.